
FOURTH-ORDER COMPACT DIFFERENCE SCHEMES FOR THE ONE-DIMENSIONAL EULER-BERNOULLI BEAM EQUATION WITH DAMPING TERM

Wenjie Huang
School of Mathematics
Sichuan University
Chengdu, China, 610065
jackson11235813@163.com

Hao Wang
School of Mathematics
Sichuan University
Chengdu, China, 610065
wangh@scu.edu.cn

Shiquan Zhang
School of Mathematics
Sichuan University
Chengdu, China, 610065
shiquanzhang@scu.edu.cn

Qinyi Zhang
School of Mathematics
Sichuan University
Chengdu, China, 610065
zqy_edu@163.com

July 1, 2025

ABSTRACT

This paper proposes and analyzes a finite difference method based on compact schemes for the Euler-Bernoulli beam equation with damping terms. The method achieves fourth-order accuracy in space and second-order accuracy in time, while requiring only three spatial grid points within a single compact stencil. Spatial discretization is carried out using a compact finite difference scheme, with a variable substitution technique employed to reduce the order of the equation and effectively handle the damping terms. For the temporal discretization, the Crank–Nicolson scheme is applied. The consistency, stability, and convergence of the proposed method are rigorously proved. Numerical experiments are presented to verify the theoretical results and demonstrate the accuracy and efficiency of the method.

Keywords Euler–Bernoulli beam equation · Compact finite difference method · Crank–Nicolson approximation · Stability analysis

1 Introduction

Euler-Bernoulli beam theory is an important theory in structural mechanics that describes the relationship between the bending moment and deflection of a beam under lateral load[1] and this type of structure is common in various industrial fields, including aviation, automobiles, railways, shipbuilding, and civil engineering[2, 3].

The core of Euler-Bernoulli beam theory is the Euler-Bernoulli beam equation, which is a fourth-order parabolic partial differential equation and is usually difficult or impossible to obtain the analytical solution[4, 5], so its numerical solution is crucial. Many people have tried to solve the Euler-Bernoulli beam equation in history and have given many numerical solutions. Ahmed provides a detailed revision of the Euler–Bernoulli and Timoshenko beam theories and their analytical and numerical applications in an appropriate and simplified manner[6].

The numerical solution of the Euler-Bernoulli equation mainly includes the finite difference method and the finite element method. Fogang applied the finite difference method (FDM) to Euler-Bernoulli beams, using the fourth-order polynomial hypothesis (FOPH) and additional points to improve accuracy, and proposed a direct time integration method (DTIM) for forced vibration analysis[7]. Twizell invented a finite difference method for numerically solving

fourth-order parabolic partial differential equations with one or two spatial variables[8]. Atilla proposed the variational derivative method to solve the Euler-Bernoulli beam functional, eliminating the need for out-of-region points in finite difference methods, and verified its performance through numerical comparisons[9]. This method is derived from the multi-derivative method of second-order ordinary differential equations. Awrejcewicz studied the chaotic vibration of a flexible nonlinear Euler-Bernoulli beam under harmonic loads and various symmetric or asymmetric boundary conditions, and verified the reliability of the results obtained by the finite difference method and the finite element method[10]. Mohanty propose a high-order compact scheme with fourth-order spatial and second-order temporal accuracy for solving 2D fourth-order PDEs, avoiding ghost points and ensuring high accuracy and stability[11]. Niiranen developed and analyzed Euler-Bernoulli beam models using strain gradient elasticity, compared different beam models, and validated their results with numerical simulations, focusing on size effects and stiffening behavior[12]. Pathak used a high-order compact finite difference scheme in MATLAB to approximate the solution of the Euler-Bernoulli beam equation for beam deflection analysis[13]. Aouragh gave a numerical solution to the undamped Euler-Bernoulli beam equation based on a compact difference scheme[14].

The finite element method is also used to solve the Euler-Bernoulli equation. Bardell introduced a hybrid h-p finite element technique for static analysis of Euler-Bernoulli beams[15]. Wei use Hermite cubic finite elements to approximate the solutions of a nonlinear Euler-Bernoulli beam equation[16]. Eltaher studied an effective finite element model for vibration analysis of nonlocal Euler-Bernoulli beams and proposed Eringen's nonlocal constitutive equations[17]. Nguyen invented a hybrid finite element method for the static analysis of nanobeams and derived the governing equations of the Euler-Bernoulli beam theory by combining nonlocal theory[18]. Shang used the generalized finite element method (GFEM) to perform dynamic analysis on one-dimensional rod and Euler-Bernoulli beam problems and analyzed the free vibration problem of beams to evaluate the robustness and efficiency of elements[19]. Zakeri used the basic displacement function (BDF) to perform structural analysis of nanobeams using the finite element method based on Eringen nonlocal elasticity and Euler Bernoulli beam theory[20]. Lin presents an error analysis of a Hermite cubic immersed finite element (IFE) method for solving interface problems of the differential equation modeling a Euler-Bernoulli beam made up of multiple materials together with suitable jump conditions at material interfaces[21]. The nonlocal Euler-Bernoulli motion equations were derived on the basis of variational statements. Wang et al. studied the displacement recovery technique through superconvergent patches and developed an adaptive finite element method for the structural characteristic problem of cracked Euler-Bernoulli beams[22]. ABRO presents a finite element numerical method for Euler-Bernoulli beams with variable coefficients[23].

Among the existing numerical methods for solving fourth-order parabolic partial differential equations, the finite difference method is favored because of its simple theoretical derivation, relatively easy implementation, flexibility and accurate numerical solution. However, the damping term is not considered in many numerical methods for solving the Euler-Bernoulli beam equation.

Therefore, the aim of our paper is to develop a numerical method to solve the Euler-Bernoulli beam equation with the damping term. This method employs a compact finite difference for the spatial derivative using a 3-point compact stencil and a second-order Crank–Nicolson approximation for the temporal derivative. Our proof to stability is general and can provide guidance to prove the stability and consistence for similar difference schemes.

The outline of this paper is as follows. In the second section, we present the process of decomposing (1) into a system of two second-order equations. Furthermore, we approximate the second-order spatial derivative using a fourth-order compact finite difference scheme, from which we obtain a system of ordinary differential equations. This system is solved using the Crank–Nicolson scheme. In the third section, we discuss the convergence, stability and convergence of the proposed scheme by the matrix method, which is shown to be unconditionally stable and second-order accurate in time and fourth-order accurate in space. In the fourth section, we present numerical results for three examples and compare errors with those from existing works in the literature, confirming the order of convergence. Finally, in the last section, we mention the conclusion of the implementation and the superiority of the proposed method based on numerical results from the problems.

2 The Damping Model And Its Compact Difference scheme

2.1 Euler-Bernoulli beam mode with damping term

We consider a one-dimensional Euler-Bernoulli beam model with damping in the domain $Q_T = [0, L] \times [0, T]$, where L is the beam length and T represents the *total time*. The problem with the model in the domain is to find $u = u(x, t)$ that satisfies the following equation with boundary conditions:

$$\begin{cases} \frac{\partial^2}{\partial x^2} \left(E(x)I(x) \frac{\partial^2 u(x,t)}{\partial x^2} \right) + \rho(x) \frac{\partial^2 u(x,t)}{\partial t^2} + c(x) \frac{\partial u(x,t)}{\partial t} = f(x,t), & (x,t) \in Q_T, \end{cases} \quad (1)$$

$$\begin{cases} u(x,0) = \xi_1(x), u_t(x,0) = \xi_2(x), \end{cases} \quad (2)$$

$$\begin{cases} u(0,t) = \mu_0(t), u(L,t) = \mu_1(t), u_{xx}(0,t) = \mu_2(t), u_{xx}(L,t) = \mu_3(t). \end{cases} \quad (3)$$

where $u_t := \frac{\partial u}{\partial t}$ and $u_{xx} := \frac{\partial^2 u}{\partial x^2}$. (2) represents the initial condition and (3) represents the boundary condition with the assumption that the beam is simply supported (or hinged) at its ends. In equation (1), u represents the displacement of a point on the beam at position x and time t relative to the equilibrium position, E represents the elastic modulus of the material, I represents the section inertia moment, ρ represents the density of material, c represents the damping coefficient, and f represents the external force. In this paper, we only consider the case where E , I , ρ , and c are all constants.

According to the first and second terms of equation (1), the solution u needs to satisfy $u \in C^4$ in the x direction and $u \in C^2$ in the t direction, and therefore we define the space

$$\mathcal{U} = \left\{ u(x,t) \in Q(x,t) \mid \frac{\partial^4 u}{\partial x^4} \text{ and } \frac{\partial^2 u}{\partial t^2} \text{ exist, } u(x,t) \text{ satisfy the equation (1), (2) and (3)} \right\} \quad (4)$$

The force term $f = f(x,t)$ is generally assumed to satisfy $f \in C^0$ since the difference schemes that this paper focuses on are required. The third term of equation (1) is also called *damping term* because it causes the dissipation of energy.

2.2 Compact difference method

We consider discretizing the problem onto a uniform grid. Let N_x, N_T be a positive integer, we uniformly divide Ω into N_x parts in x direction and N_T parts in t direction, denote the step size of spatial variable x by $h = \Delta x = \frac{L}{N_x}$ and the step size of time variable t by $\Delta t = \frac{T}{N_T}$, and write $(\Delta x)^y, (\Delta t)^y$ as $\Delta x^y, \Delta t^y$. We denote the corresponding admissible set of spatial coordinates by $\mathbf{X} := \{0, 1, \dots, N_x\}$ and time coordinates by $\mathbf{T} := \{0, 1, \dots, N_T\}$. For a function $v \in \mathcal{U}$, we define the finite difference operators

$$\delta_k^c v_i^n := \sum_{j=-k}^k \hat{b}_j v_{i+j}^n, \quad (5)$$

where \hat{b}_j is fixed corresponding to center difference scheme when N, c are fixed, and $v_i^n = v(i\Delta x, n\Delta t), i \in \mathbf{X}, n \in \mathbf{T}$. Again, we define compact difference operators of c -order derivative

$$D_N^c v_i^n := \sum_{j=-N}^N a_j \left(\frac{\partial^c v}{\partial x^c} \right)_{i+j}^n, \quad a_j > 0, \quad N \leq i \leq N_x - N. \quad (6)$$

where a_j represents the weight of the term in compact scheme and notice that the number of points we used is $2N + 1$ by definition (6). Now the compact difference scheme of c -order derivative is able to be expressed in the form of

$$D_N^c v_i^n = \frac{1}{\Delta x^c} \sum_{j=1}^{\hat{N}} b_j \delta_j^c v_i^n, \quad (7)$$

the integer N, \hat{N} is defined to satisfies the consistence

$$D_N^c v_i^n - \frac{1}{\Delta x^c} \sum_{j=1}^{\hat{N}} b_j \delta_j^c v_i^n = O(\Delta x^k). \quad (8)$$

where k is fixed and (7)-(8) mean that we use finite difference scheme to approximate the weighted average of the derivatives of multiple points instead of the derivative of one point. The advantage of this is that a higher order of convergence can be obtained with fewer discrete points, especially in some cases of uniform grid. We use Taylor series to deduce the the integer N, \hat{N} with a fixed appropriate integer k .

For convenience, we also define a operator \tilde{D}_N^c :

$$\tilde{D}_N^c v_i^n := \sum_{j=-N}^N a_j v_{i+j}^n, \quad a_j > 0, \quad N \leq i \leq N_x - N. \quad (9)$$

where a_j is the coefficient of $D_N^c v_i^n$ defined by (6). That means we ignore the differential effect when we use the operator \tilde{D}_N^c which corresponds to operator D_N^c .

In this paper, the scheme we used of second derivative with $k = 4$ is

$$D_1^2 v_i^n = \frac{1}{\Delta x^2} \delta_1^2 v_i^n, \quad (10)$$

here we choose $N = 1$, $\hat{N} = 1$ for $k = 4$ and expand (10) in uniform grid with $b_1 = 1$ and $a_1 = a_{-1} = 1/12$, $a_0 = 5/6$

$$\frac{1}{12} \left(\frac{\partial^2 v}{\partial x^2} \right)_{i+1}^n + \frac{5}{6} \left(\frac{\partial^2 v}{\partial x^2} \right)_i^n + \frac{1}{12} \left(\frac{\partial^2 v}{\partial x^2} \right)_{i-1}^n = \frac{1}{\Delta x^2} \delta_1^2 v_i^n. \quad (11)$$

With the scheme above, we can discrete the equation and solve it.

2.3 Compact difference scheme separating first and second time derivatives

First, we replace the variables with the following form and transform the fourth-order equation into a second-order equation system,

$$\begin{cases} \phi(x, t) = u_t(x, t), \\ \psi(x, t) = u_{xx}(x, t). \end{cases} \quad (12)$$

Then equation (1) turns to

$$\begin{cases} EI\psi_{xx}(x, t) = -\rho\phi_t(x, t) - c\phi(x, t) - f(x, t), \\ \phi_{xx}(x, t) = \psi_t(x, t). \end{cases} \quad (13)$$

$$(14)$$

In the variable substitution, $\phi(x, t)$ represents the velocity of the beam, and $\psi(x, t)$ represents the bending moment value of the beam. For simplicity in analysis, we rewrite the equation (13)-(14) with operators in the following form:

$$\mathcal{L}H = \mathcal{F}, \quad (15)$$

where $H = H(\phi, \psi)$ and \mathcal{F} represents the force term. Exactly \mathcal{L} is a vector operator with two components

$$\mathcal{L} = \begin{pmatrix} \bar{\mathcal{L}} \\ \bar{\bar{\mathcal{L}}} \end{pmatrix}, \quad (16)$$

where

$$\bar{\mathcal{L}}(\phi, \psi) = -EI\psi_{xx} - \rho\phi_t - c\phi, \quad (17)$$

$$\bar{\bar{\mathcal{L}}}(\phi, \psi) = \phi_{xx} - \psi_t. \quad (18)$$

To get an spatial semidiscrete scheme we apply compact difference scheme (7) to (13), notice that here $c = 2$

$$D_1^2 \psi_i^n = \frac{1}{\Delta x^2} \delta_1^2 \psi_i^n, \quad (19)$$

by the definition of compact scheme

$$D_1^2 EI\psi_i^n = \tilde{D}_1^2 (f - \rho\phi_t - c\phi)_i^n, \quad (20)$$

Where a_j is already given by left terms of equation (11). And apply the same way to (14) and notice that

$$D_1^2 \phi_i^n = \tilde{D}_1^2 (\psi_t)_i^n. \quad (21)$$

We deduce the compact scheme of equation system (13)-(14) by combining (19)-(20) and (21)

$$\begin{cases} \tilde{D}_1^2 (f - \rho\phi_t - c\phi)_i^n = \frac{1}{\Delta x^2} \delta_1^2 EI\psi_i^n, \\ \tilde{D}_1^2 (\psi_t)_i^n = \frac{1}{\Delta x^2} \delta_1^2 \phi_i^n, \end{cases} \quad (22)$$

$$(23)$$

rewrite (22) and (23) as systems of ordinary differential equations and implies

$$\begin{cases} \mathbf{A}(\rho\Phi_t + c\Phi - \mathbf{f}) = \mathbf{B}\Psi, \\ \mathbf{A}\Psi_t = -\mathbf{B}\Phi, \end{cases} \quad (24)$$

$$(25)$$

where we define

$$\mathbf{\Phi} := (\phi_1, \phi_2, \dots, \phi_{N_x-1})^T, \mathbf{\Psi} := (\psi_1, \psi_2, \dots, \psi_{N_x-1})^T, \mathbf{f} := (f_1, f_2, \dots, f_{N_x-1})^T, \quad (26)$$

$$\mathbf{\Phi}_t := \frac{\partial}{\partial t} \mathbf{\Phi} = \left(\left(\frac{\partial \phi}{\partial t} \right)_1, \left(\frac{\partial \phi}{\partial t} \right)_2, \dots, \left(\frac{\partial \phi}{\partial t} \right)_{N_x-1} \right)^T, \mathbf{\Psi}_t := \frac{\partial}{\partial t} \mathbf{\Psi} = \left(\left(\frac{\partial \psi}{\partial t} \right)_1, \left(\frac{\partial \psi}{\partial t} \right)_2, \dots, \left(\frac{\partial \psi}{\partial t} \right)_{N_x-1} \right)^T, \quad (27)$$

where $\phi_i(t) = \phi(i\Delta x, t)$, the coefficient matrix \mathbf{A}, \mathbf{B} is given by the following equation

$$\mathbf{A} := \text{diag}_{N_x-1} \left(\frac{1}{12}, \frac{5}{6}, \frac{1}{12} \right), \quad (28)$$

$$\mathbf{B} := \frac{1}{\Delta x^2} \text{diag}_{N_x-1} (-1, 2, -1). \quad (29)$$

the $\text{diag}_{N_x-1}(a_{-1}, a_0, a_1)$ is redefined here as tridiagonal matrix of $(N_x - 1) \times (N_x - 1)$ size:

$$\text{diag}_{N_x-1}(a_{-1}, a_0, a_1) := \begin{pmatrix} a_0 & a_1 & & & & \\ a_{-1} & a_0 & a_1 & & & \\ & a_{-1} & a_0 & a_1 & & \\ & & & \dots & & \\ & & & a_{-1} & a_0 & a_1 \\ & & & & a_{-1} & a_0 & a_1 \\ & & & & & a_{-1} & a_0 \end{pmatrix}_{(N_x-1) \times (N_x-1)} \quad (30)$$

Notice that (24)-(25) can be organized into one linear system by combining $\mathbf{\Phi}$ and $\mathbf{\Psi}$ into a new vector, i.e.

$$\mathbf{A}\mathbf{U}_t = \mathbf{B}\mathbf{U} + \mathbf{F}, \quad (31)$$

where

$$\mathbf{U} := \begin{pmatrix} \mathbf{\Phi} \\ \mathbf{\Psi} \end{pmatrix}, \mathbf{U}_t := \frac{\partial}{\partial t} \mathbf{U} = \begin{pmatrix} \mathbf{\Phi}_t \\ \mathbf{\Psi}_t \end{pmatrix}, \mathbf{F} := \begin{pmatrix} \mathbf{F}_1 \\ \mathbf{F}_2 \end{pmatrix}, \quad (32)$$

$$\mathbf{A} := \begin{pmatrix} \rho \mathbf{A} & \mathbf{0} \\ \mathbf{0} & \mathbf{A} \end{pmatrix}, \mathbf{B} := \begin{pmatrix} -c \mathbf{A} & E \mathbf{I} \mathbf{B} \\ -\mathbf{B} & \mathbf{0} \end{pmatrix}, \quad (33)$$

and

$$\mathbf{F}_1 = \left(\alpha + \tilde{D}_1^2 f_1, \tilde{D}_1^2 f_2, \dots, \tilde{D}_1^2 f_{N_x-2}, \tilde{D}_1^2 f_{N_x-1} + \beta \right)^T, \\ \mathbf{F}_2 = (\alpha', 0, \dots, 0, \beta')^T,$$

where $\alpha, \beta, \alpha', \beta'$ represents the boundary condition:

$$\alpha = -EI \frac{\psi_0(t)}{h^2} - \rho \frac{\phi'_0(t)}{12} - c \frac{\phi_0(t)}{12}, \\ \beta = -EI \frac{\psi_{N_x}(t)}{h^2} - \rho \frac{\phi'_{N_x}(t)}{12} - c \frac{\phi_{N_x}(t)}{12}, \\ \alpha' = \frac{\phi_0(t)}{h^2} - \frac{\psi'_0(t)}{12}, \\ \beta' = \frac{\phi_{N_x}(t)}{h^2} - \frac{\psi'_{N_x}(t)}{12}.$$

In order to maintain the stability in time, we use Crank-Nicolson scheme[24], which yields

$$\mathbf{A} \left(\frac{\mathbf{U}^{n+1} - \mathbf{U}^n}{\Delta t} \right) = \mathbf{B} \left(\frac{\mathbf{U}^{n+1} + \mathbf{U}^n}{2} \right) + \left(\frac{\mathbf{F}^{n+1} + \mathbf{F}^n}{2} \right). \quad (34)$$

We can rewrite the difference scheme above the same as (15) in point-to-point form

$$\mathcal{L}_j^n H_j^n = G_j^n, \quad (35)$$

where $H_j^n = H(\phi_j^n, \psi_j^n)$ and G_j^n represents the force term. Notice that \mathcal{L}_j^n is the same as \mathcal{L} and also has two components

$$\mathcal{L}_j^n = \begin{pmatrix} \bar{\mathcal{L}}_j^n \\ \bar{\bar{\mathcal{L}}}_j^n \end{pmatrix}, \quad (36)$$

where

$$\begin{aligned} \bar{\mathcal{L}}_j^n H_j^n &:= \frac{\rho}{\Delta t} \tilde{D}_1^2 (\phi_i^{n+1} - \phi_i^n) + \frac{c}{2} \tilde{D}_1^2 (\phi_i^{n+1} + \phi_i^n) + \frac{EI}{2\Delta x^2} (\delta_1^2 \psi_i^{n+1} + \delta_1^2 \psi_i^n), \\ \bar{\bar{\mathcal{L}}}_j^n &:= \frac{1}{2} \tilde{D}_1^2 (f_i^{n+1} + f_i^n). \end{aligned}$$

and

$$\begin{aligned} \bar{\bar{\mathcal{L}}}_j^n H_j^n &:= \frac{1}{\Delta t} \tilde{D}_1^2 (\psi_i^{n+1} - \psi_i^n) - \frac{1}{2} \tilde{D}_1^2 (\phi_i^{n+1} + \phi_i^n), \\ \bar{\bar{\bar{\mathcal{L}}}}_j^n &:= 0 \end{aligned}$$

which are the point-by-point form corresponding to (34).

Since matrix \mathcal{A} is invertible, the equation (34) can be rewritten as

$$\left(\mathbf{I} - \frac{\Delta t}{2} \mathcal{A}^{-1} \mathcal{B} \right) \mathbf{U}^{n+1} = \left(\mathbf{I} + \frac{\Delta t}{2} \mathcal{A}^{-1} \mathcal{B} \right) \mathbf{U}^n + \frac{\Delta t}{2} \mathcal{A}^{-1} (\mathbf{F}^{n+1} + \mathbf{F}^n). \quad (37)$$

Solving the above equation yields vector \mathbf{U}^n , noting that vector $\mathbf{\Psi}^n \in \mathbf{U}^n$ is the second-order spatial derivative of the original solution from (12), and recall the compact difference scheme with $c = 2$

$$D_1^2 u_i^n = \frac{1}{\Delta x^2} \delta_1^2 u_i^n, \quad (38)$$

$$(39)$$

again, rewrite it as a linear system using the matrix \mathbf{A} and \mathbf{B}

$$\mathbf{A} \mathbf{\Psi}^n = -\mathbf{B} \mathbf{C}^n. \quad (40)$$

where $\mathbf{C}^n := (u_1^n, \dots, u_{N_x-1}^n)^T$.

3 Consistency, Stability and Convergence

In this section, we give analytical proof of the consistency, stability and convergence of the difference scheme (34), thereby demonstrating that the difference scheme has excellent properties.

3.1 Consistency Analysis

Before proving the consistency of the final scheme and the original equation, we shall prove the consistency of (35) first.

Lemma 1. *The compact scheme (35) is pointwise consistent with the partial differential equation (15) at point (x, t) and*

$$\|(\mathcal{L}H - F)_j^n - (\mathcal{L}_j^n H_j^n - G_j^n)\|_\infty = O(\Delta x^4) + O(\Delta t^2). \quad (41)$$

Proof. Note that the scheme (35) has two part schemes so we first expand $\bar{\mathcal{L}}_j^n H_j^n - \bar{G}_j^n$ into Taylor series at point (x, t) , we have

$$\bar{\mathcal{L}}_j^n H_j^n - \bar{G}_j^n = c\phi_j^{n+1} + \rho \left(\frac{\partial \phi}{\partial t} \right)_j^{n+1} + EI \left(\frac{\partial^2 \psi}{\partial x^2} \right)_j^{n+1} - f_j^{n+1} \quad (42)$$

$$- \frac{\Delta t}{2} \left[c \left(\frac{\partial \phi}{\partial t} \right)_j^{n+1} + \rho \left(\frac{\partial^2 \phi}{\partial t^2} \right)_j^{n+1} + EI \left(\frac{\partial^3 \psi}{\partial t \partial x^2} \right)_j^{n+1} - \left(\frac{\partial f}{\partial t} \right)_j^{n+1} \right] \quad (43)$$

$$+ \frac{(\Delta x)^2}{12} \left[c \left(\frac{\partial^2 \phi}{\partial x^2} \right)_j^{n+1} + \rho \left(\frac{\partial^3 \phi}{\partial t \partial x^2} \right)_j^{n+1} + EI \left(\frac{\partial^4 \psi}{\partial x^4} \right)_j^{n+1} - \left(\frac{\partial^2 f}{\partial x^2} \right)_j^{n+1} \right] \quad (44)$$

$$- \frac{\Delta t (\Delta x)^2}{24} \left[c \left(\frac{\partial^3 \phi}{\partial t \partial x^2} \right)_j^{n+1} + \rho \left(\frac{\partial^4 \phi}{\partial t^2 \partial x^2} \right)_j^{n+1} + EI \left(\frac{\partial^5 \psi}{\partial t \partial x^4} \right)_j^{n+1} - \left(\frac{\partial^3 f}{\partial t \partial x^2} \right)_j^{n+1} \right] \quad (45)$$

$$+ O(\Delta t^2) + O(\Delta x^4), \quad (46)$$

and then use the equation (13) to eliminate the relevant terms to obtain

$$\bar{\mathcal{L}}_j^n H_j^n - \bar{G}_j^n = O(\Delta x^4) + O(\Delta t^2). \quad (47)$$

We can get the following result by similar derivation to the second scheme

$$\bar{\bar{\mathcal{L}}}_j^n H_j^n - \bar{\bar{G}}_j^n = O(\Delta x^4) + O(\Delta t^2). \quad (48)$$

Combining (47) and (48) leads to the consistence:

$$\left\| (\mathcal{L}H - F)_j^n - (\mathcal{L}_j^n H_j^n - G_j^n) \right\|_\infty = \left\| \left((\bar{\mathcal{L}}H - \bar{F})_j^n - (\bar{\mathcal{L}}_j^n H_j^n - \bar{G}_j^n) \right) \right\|_\infty \quad (49)$$

$$= \max\{(\bar{\mathcal{L}}H - \bar{F})_j^n - (\bar{\mathcal{L}}_j^n H_j^n - \bar{G}_j^n), (\bar{\bar{\mathcal{L}}}H - \bar{\bar{G}})_j^n - (\bar{\bar{\mathcal{L}}}_j^n H_j^n - \bar{\bar{G}}_j^n)\} \quad (50)$$

$$= O(\Delta x^4) + O(\Delta t^2). \quad (51)$$

□

It shows the scheme (34) is second-order accurate in time and fourth-order accurate in space.

Theorem 1 (Consistency). *The final scheme is pointwise consistent with the origin equation (1) and is second-order accurate in time and fourth-order accurate in space.*

Proof. It is natural to deduce that scheme (39) is consistent with the equation

$$u_{xx}(x, t) = \psi(x, t). \quad (52)$$

since (10) has already ensured it and is fourth-order accurate in space. From lemma 1 we know that scheme (35) is consistent with equations (13), which is actually transformed from equation (1), so we must have the final scheme where we get numerical solution $u(x_i, t_n)$ is pointwise consistent with the origin equation (1), and is second-order accurate in time and fourth-order accurate in space. □

3.2 Stability Analysis

Since the right end term matrix of (37) has no effect on the stability of the scheme, we will simplify the equation to the following form when analyzing its stability

$$\mathcal{Q}_1 U^{n+1} = \mathcal{Q}_2 U^n. \quad (53)$$

here we denote

$$\mathcal{Q}_1 = \left(\mathbf{I} - \frac{\Delta t}{2} \mathcal{A}^{-1} \mathcal{B} \right), \quad (54)$$

$$\mathcal{Q}_2 = \left(\mathbf{I} + \frac{\Delta t}{2} \mathcal{A}^{-1} \mathcal{B} \right), \quad (55)$$

and the amplification matrix \mathcal{Q} is given by

$$\mathcal{Q} = \mathcal{Q}_1^{-1} \mathcal{Q}_2. \quad (56)$$

In order to obtain the stability of the scheme proposed in the previous section, we need to verify whether the spectral radius of the amplification matrix satisfies the von Neumann stability condition, that is, to verify

$$|\rho(\mathcal{Q})| = \sup_{\mathcal{Q}\mathbf{x}=\lambda\mathbf{x}, \mathbf{x} \neq \mathbf{0}} |\lambda| \leq 1. \quad (57)$$

where $\rho(\mathcal{Q})$ represents the spectral radius of \mathcal{Q} .

We now give a general statement and proof of the above discussion. First we will introduce some useful lemmas

Lemma 2. *All of the eigenvalues of a real symmetric and strictly diagonally dominant matrix with positive diagonal elements are positive real numbers.*

Proof. Let $\mathbf{\Lambda}$ be a real symmetric and strictly diagonally dominant matrix with n rows and n columns, and let η be the eigenvalue of $\mathbf{\Lambda}$ with eigenvector \mathbf{x} i.e. $\mathbf{\Lambda}\mathbf{x} = \eta\mathbf{x}$.

For $n = 1, 2$ the result is trivial.

Here we consider the situation with $n \geq 3$. First η must be a real number since $\mathbf{\Lambda}$ is real symmetric. Using the Gershgorin Circle Theorem[25], we can deduce the estimate of η , and notice that $\mathbf{\Lambda}$ is strictly diagonally dominant i.e.

$$\sum_{j=1, j \neq i}^n |\Lambda_{ij}| < |\Lambda_{ii}|, \quad (58)$$

so

$$|\Lambda_{ii} - \eta| \leq \sum_{j=1, j \neq i}^n |\Lambda_{ij}| < |\Lambda_{ii}|, \quad (59)$$

here Λ_{ij} denote the element of i th row and j th column. since $\Lambda_{ii} > 0$, (59) holds if only if $\eta > 0$ holds. \square

Lemma 3. *The relation (57) holds if and only if $\Re(z) \leq 0$, where z is the eigenvalue of matrix $\mathcal{A}^{-1}\mathcal{B}$.*

Proof. First, we let $\lambda, \lambda_1, \lambda_2$, and z be eigenvalues of $\mathcal{Q}, \mathcal{Q}_1, \mathcal{Q}_2$, and $\mathcal{A}^{-1}\mathcal{B}$, respectively. From the definition of \mathcal{Q} implies

$$\lambda = \frac{\lambda_2}{\lambda_1}, \quad (60)$$

since $(\hat{\mathbf{A}} \pm k\mathbf{I})\mathbf{x} = (\hat{\lambda} \pm k)\mathbf{x}$, for any complex number k , and $\hat{\mathbf{A}}\mathbf{x} = \hat{\lambda}\mathbf{x}$. We deduce

$$\lambda_1 = 1 - \frac{\Delta t}{2}z, \quad (61)$$

$$\lambda_2 = 1 + \frac{\Delta t}{2}z, \quad (62)$$

combine the results above implies

$$\lambda = \frac{1 + \frac{\Delta t}{2}z}{1 - \frac{\Delta t}{2}z}. \quad (63)$$

Let's set $z\Delta t = a + bi$ where $a, b \in \mathbb{R}$. A simple computation yields

$$|\lambda_1|^2 = (1 + \frac{a}{2})^2 + \frac{b^2}{4}, \quad (64)$$

and

$$|\lambda_2|^2 = (1 - \frac{a}{2})^2 + \frac{b^2}{4}. \quad (65)$$

From these calculations, we observe that $|\lambda_1| \leq |\lambda_2|$ if and only if $a \leq 0$ and $|\lambda_1| > |\lambda_2|$ if and only if $a > 0$. Therefore, the relation (57) holds if and only if z be in the left-half complex plane, that is $\Re(z) \leq 0$. \square

Now we only need to prove that all the eigenvalues of $\mathcal{A}^{-1}\mathcal{B}$ have a negative real part. Before proof it, we should proof a lemma.

Lemma 4. *The matrices $A = \text{diag}_n(b, a, b)$ and $B = \text{diag}_n(d, c, d)$ are commutative.*

Proof. We proceed by induction on the size of the matrices A and B .

First, for $n = 1$, the conclusion is trivial.

For $n = 2$, through direct computation, we have

$$AB = \begin{pmatrix} a & b \\ b & a \end{pmatrix} \begin{pmatrix} c & d \\ d & c \end{pmatrix} = \begin{pmatrix} ac + bd & ad + bc \\ bc + ad & bd + ac \end{pmatrix} = \begin{pmatrix} c & d \\ d & c \end{pmatrix} \begin{pmatrix} a & b \\ b & a \end{pmatrix} = BA. \quad (66)$$

Assume that the conclusion holds for $n - 1$, for the case of n ,

$$A = \begin{pmatrix} A_1 & \alpha \\ \alpha^T & a \end{pmatrix}, B = \begin{pmatrix} B_1 & \beta \\ \beta^T & c \end{pmatrix}, \quad (67)$$

where $\alpha = (0, \dots, b)^T \in \mathbb{C}^{n-1}$, $\beta = (0, \dots, d)^T \in \mathbb{C}^{n-1}$, $A_1 = \text{diag}\{b, a, b\}_{n-1}$, and $B_1 = \text{diag}\{d, c, d\}_{n-1}$. Computing the products, we obtain

$$AB = \begin{pmatrix} A_1 & \alpha \\ \alpha^T & a \end{pmatrix} \begin{pmatrix} B_1 & \beta \\ \beta^T & c \end{pmatrix} = \begin{pmatrix} A_1 B_1 + \alpha \beta^T & A_1 \beta + c \alpha \\ \alpha^T B_1 + a \alpha^T & \alpha^T \beta + ac \end{pmatrix}, \quad (68)$$

and

$$BA = \begin{pmatrix} B_1 & \beta \\ \beta^T & c \end{pmatrix} \begin{pmatrix} A_1 & \alpha \\ \alpha^T & a \end{pmatrix} = \begin{pmatrix} B_1 A_1 + \beta \alpha^T & B_1 \alpha + a \beta \\ \beta^T A_1 + c \alpha^T & \beta^T \alpha + ca \end{pmatrix}. \quad (69)$$

Since both α and β are vectors, it follows that $\alpha \beta^T = \beta \alpha^T$ and $\alpha^T \beta = \beta^T \alpha$. By the induction hypothesis, we know that $A_1 B_1 = B_1 A_1$. Thus, we have

$$A_1 B_1 + \alpha \beta^T = B_1 A_1 + \beta \alpha^T, \quad (70)$$

$$\alpha^T \beta + ac = \beta^T \alpha + ca. \quad (71)$$

Moreover, direct computation yields

$$A_1 \beta + c \alpha = B_1 \alpha + a \beta = (0, \dots, bd, ad + bc)^T, \quad (72)$$

$$\alpha^T B_1 + a \alpha^T = \beta^T A_1 + c \alpha^T = (0, \dots, bd, ad + bc). \quad (73)$$

Therefore, it follows that $AB = BA$. By the principle of induction, the lemma is proved. \square

Remark 1. *From the above lemma, we know that the matrices \mathbf{A} and \mathbf{B} , as defined in the finite difference method, are commutative, i.e., $\mathbf{AB} = \mathbf{BA}$. Since \mathbf{A} is invertible, we multiply both sides of the equation $\mathbf{AB} = \mathbf{BA}$ on the left by \mathbf{A}^{-1} and on the right by \mathbf{A}^{-1} , yielding $\mathbf{A}^{-1}\mathbf{B} = \mathbf{BA}^{-1}$.*

Lemma 5. *If EI, ρ and c are all positive numbers, then all the eigenvalues of $\mathcal{A}^{-1}\mathcal{B}$ have negative real part.*

Proof. Let $\eta = x + iy$ be an eigenvalue of the matrix $\mathcal{C} := \mathcal{A}^{-1}\mathcal{B}$ and $\zeta = \begin{pmatrix} \zeta_1 \\ \zeta_2 \end{pmatrix}$ be the corresponding non-zero eigenvector, where $\zeta \in \mathbb{C}^{2(N_x-1)}$, $\zeta_1, \zeta_2 \in \mathbb{C}^{N_x-1}$, i.e.

$$\mathcal{C}\zeta = \mathcal{A}^{-1}\mathcal{B}\zeta = \begin{pmatrix} \frac{1}{\rho}\mathbf{A}^{-1} & \mathbf{0} \\ \mathbf{0} & \mathbf{A}^{-1} \end{pmatrix} \begin{pmatrix} -c\mathbf{A} & EIB \\ -\mathbf{B} & \mathbf{0} \end{pmatrix} \zeta = \begin{pmatrix} -\frac{c}{\rho}\mathbf{I} & \frac{EI}{\rho}\mathbf{A}^{-1}\mathbf{B} \\ -\mathbf{A}^{-1}\mathbf{B} & \mathbf{0} \end{pmatrix} \zeta = \eta\zeta. \quad (74)$$

So we have two equation of ζ_1 and ζ_2

$$\begin{cases} -\frac{c}{\rho}\zeta_1 + \frac{EI}{\rho}\mathbf{A}^{-1}\mathbf{B}\zeta_2 = \eta\zeta_1, \\ -\mathbf{A}^{-1}\mathbf{B}\zeta_1 = \eta\zeta_2. \end{cases}$$

Then the relation between ζ_1 and ζ_2 is

$$\mathbf{A}^{-1}\mathbf{B}\zeta_2 = \frac{\rho\eta + c}{EI}\zeta_1. \quad (75)$$

Take the conjugate transpose on both sides of the equation (74) gives $\zeta^* \mathcal{C}^* = \bar{\eta} \zeta^*$. Right multiply vector ζ , we have

$$\zeta^* \mathcal{C}^* \zeta = \bar{\eta} \zeta^* \zeta. \quad (76)$$

Left multiply equation (74) with vector ζ^* , we have

$$\zeta^* \mathcal{C} \zeta = \eta \zeta^* \zeta. \quad (77)$$

Note that \mathbf{A}^{-1} , \mathbf{B} are both symmetric matrices. We also know $\mathbf{A}^{-1} \mathbf{B} = \mathbf{B} \mathbf{A}^{-1}$ from remark 1, so we have

$$\mathcal{C}^* = \begin{pmatrix} -\frac{c}{\rho} \mathbf{I} & -\mathbf{A}^{-1} \mathbf{B} \\ \frac{EI}{\rho} \mathbf{A}^{-1} \mathbf{B} & \mathbf{0} \end{pmatrix} \quad (78)$$

So add equation (76) and (77) side by side, and use the relation (75), we can perform the following calculation

$$\begin{aligned} \zeta^* (\mathcal{C}^* + \mathcal{C}) \zeta &= \begin{pmatrix} \zeta_1^* & \zeta_2^* \end{pmatrix} \begin{pmatrix} -\frac{2c}{\rho} \mathbf{I} & (\frac{EI}{\rho} - 1) \mathbf{A}^{-1} \mathbf{B} \\ (\frac{EI}{\rho} - 1) \mathbf{A}^{-1} \mathbf{B} & \mathbf{0} \end{pmatrix} \begin{pmatrix} \zeta_1 \\ \zeta_2 \end{pmatrix} \\ &= -\frac{2c}{\rho} \zeta_1^* \zeta_1 + \left(\frac{EI}{\rho} - 1 \right) \zeta_1^* \mathbf{A}^{-1} \mathbf{B} \zeta_2 + \left(\frac{EI}{\rho} - 1 \right) \zeta_2^* \mathbf{A}^{-1} \mathbf{B} \zeta_1 \\ &= -\frac{2c}{\rho} \zeta_1^* \zeta_1 + 2\Re \left[\left(\frac{EI}{\rho} - 1 \right) \zeta_1^* \mathbf{A}^{-1} \mathbf{B} \zeta_2 \right] \\ &= -\frac{2c}{\rho} \zeta_1^* \zeta_1 + 2 \left(\frac{EI}{\rho} - 1 \right) \Re [\zeta_1^* \mathbf{A}^{-1} \mathbf{B} \zeta_2] \\ &= -\frac{2}{\rho} \{ c \zeta_1^* \zeta_1 + (\rho - EI) \Re [\zeta_1^* \mathbf{A}^{-1} \mathbf{B} \zeta_2] \} \\ &= -\frac{2}{\rho} \left[c + \left(\frac{\rho}{EI} - 1 \right) \Re(\rho\eta + c) \right] \zeta_1^* \zeta_1 \\ &= -2 \left[\left(\frac{\rho}{EI} - 1 \right) \Re(\eta) + \frac{c}{EI} \right] \zeta_1^* \zeta_1 \\ &= (\eta + \bar{\eta}) \zeta^* \zeta \\ &= 2\Re(\eta) \zeta^* \zeta, \end{aligned}$$

Taking the last formula and the third to last formula of calculation above, we have

$$\left[\left(1 - \frac{\rho}{EI} \right) \Re(\eta) - \frac{c}{EI} \right] \zeta_1^* \zeta_1 = \Re(\eta) \zeta^* \zeta,$$

Note that $\zeta^* \zeta = \zeta_1^* \zeta_1 + \zeta_2^* \zeta_2$, then we have

$$-\left(\frac{\rho}{EI} \zeta_1^* \zeta_1 + \zeta_2^* \zeta_2 \right) \Re(\eta) = \frac{c}{EI} \zeta_1^* \zeta_1.$$

It's easy to note that $\zeta_1^* \zeta_1 \geq 0$ and $\zeta_2^* \zeta_2 \geq 0$. And by assumption, so we must have $\Re(\eta) \leq 0$. \square

Remark 2. The conditions in the theorem are that E, ρ, c are all positive numbers, and in the actual physical background, these values are all positive numbers. Therefore, we have proved the stability of this method in general engineering calculations.

Remark 3. Note that if only the real part of the eigenvalue of \mathcal{B} is less than or equal to 0, it cannot be obtained that the real part of the eigenvalue of $\mathbf{A}^{-1} \mathcal{B}$ is less than or equal to 0, where \mathcal{A} is defined by (33). For example, let $EI = \rho = c = 1$, and \mathcal{A}, \mathcal{B} are both fourth-order matrices, where

$$\mathcal{B} = \begin{bmatrix} -3 & -4 & 3 & -2 \\ 5 & 0 & 0 & 2 \\ 4 & -1 & -1 & 5 \\ -2 & 5 & -4 & -2 \end{bmatrix}$$

then we can compute that the eigenvalues of \mathcal{B} and $\mathbf{A}^{-1} \mathcal{B}$ are It can be found that the real part of the eigenvalues of \mathcal{B} is less than or equal to 0, but $\mathbf{A}^{-1} \mathcal{B}$ is not in table (1). Therefore, the proofs of stability analysis in many literature are completely wrong, such as [14].

According to the above discussion, we get the following theorem

Theorem 2 (Stability). If E, I, ρ, c are all positive constants, then the scheme (34) is unconditionally stable.

Eigenvalues of \mathcal{B}	Eigenvalues of $\mathcal{A}^{-1}\mathcal{B}$
$-4.2503 + 0.0000i$	$-6.4027 + 0.0000i$
$-1.3154 + 0.0000i$	$-1.2627 + 0.0000i$
$-0.2172 + 4.1164i$	$0.0751 + 4.9855i$
$-0.2172 - 4.1164i$	$0.0751 - 4.9855i$

Table 1: Eigenvalues of \mathcal{B} and $\mathcal{A}^{-1}\mathcal{B}$

3.3 Convergence Analysis

Now we have proven the stability of the scheme. The convergence of the numerical scheme can be concluded using the Lax Richtmyer theorem: stability and consistency imply convergence[26]. So now we have the convergence theorem below:

Theorem 3 (Convergence). *Let $u(x, t) \in \mathcal{U}$ be the analytical solution of the Euler-Bernoulli beam equation, and assume u_{xxxx} and u_{tt} are bounded in the domain. The compact difference scheme is convergence with infinity-norm, further,*

$$\|\mathbf{u}^n - \mathbf{v}^n\|_{l^\infty} = O(\Delta x^4) + O(\Delta t^2), n \in \mathbf{T}, \quad (79)$$

where \mathbf{u}^n and \mathbf{v}^n represent the solution vector of numerical solution and exact solution at n -th time step, respectively.

4 Numerical Experiments

In this section, we present the numerical results of the proposed method applied to three examples of beam equations existing in the literature. We note that all calculations are achieved using the JULIA language on a MacBook Pro computer equipped with the processor 1,8 GHz Intel Core i5. We test the accuracy and stability of the proposed method by using it with different values of Δt and h . The L^∞ error obtained for the method is shown. We also calculate the computational orders of our method (denoted by *C-Order*) using the following formula

4.1 Example 1

Example 1. Set $EI = 98, \rho = 0.685, c = 0.75$ in model (1) to (3) and the force term f is chosen such that exact solution is

$$u(x, t) = \sin(\pi x) \cos(\pi t). \quad (80)$$

The exact solution ,numerical solution and error between exact and numerical solution, are plotted on 2D for $h = 0.01$ and $t = 0.005$ in fig 1. The maximum absolute errors in the solution u and convergence in time of example 1, are listed in Table 2 for different values of h at $t = 1$. Fig 4.1 and 4.1 show the convergence order of Example 1 in space and time, respectively.

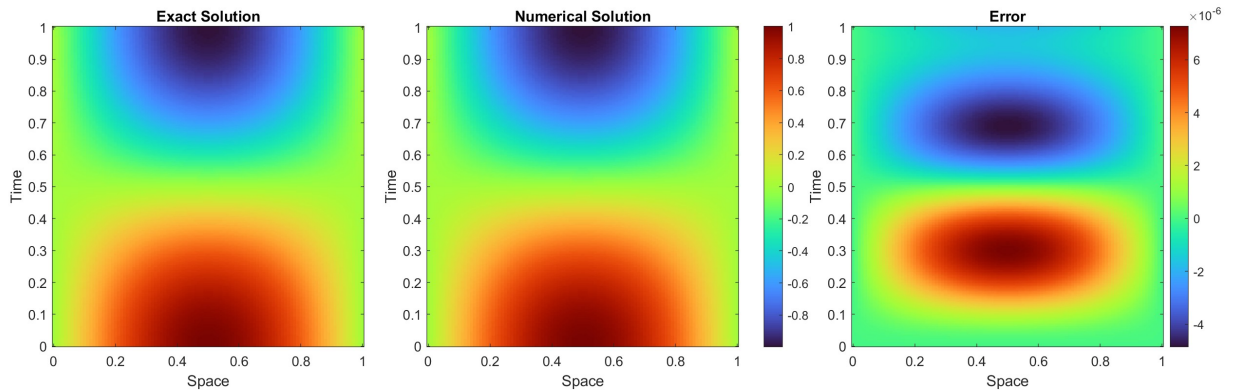
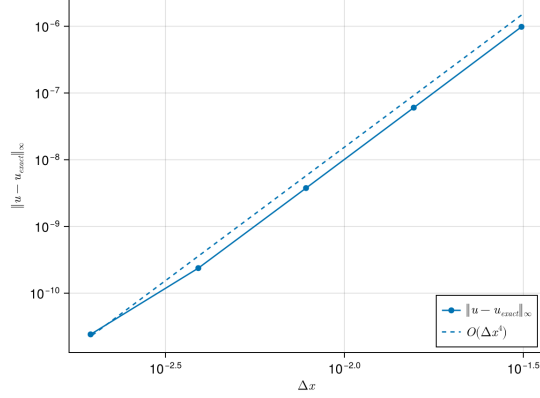
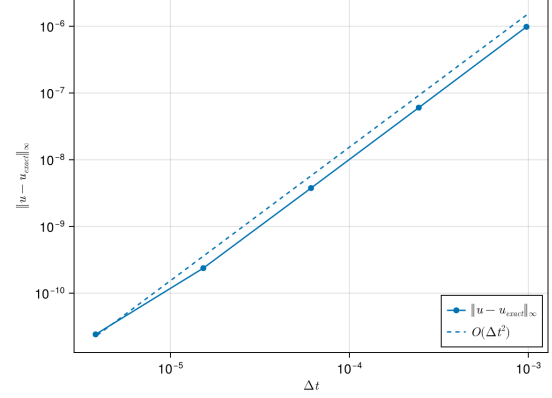


Figure 1: Example 1: Exact solution (left), Numerical solution (middle) and Error (right) for $h = 0.01$ and $\Delta t = 0.005$

Mesh	N	h	e_h	C -order
$Mesh_1$	32	0.0312	6.634501648061786e-7	-
$Mesh_2$	64	0.0156	4.1534138461862824e-8	3.997618567152459
$Mesh_3$	128	0.0078	2.597110193569563e-9	3.999318496099914
$Mesh_4$	256	0.0039	1.6252299506192003e-10	3.9981914660506632
$Mesh_5$	512	0.0020	1.0099698855015049e-11	4.008259675123924
Average				4.000847051

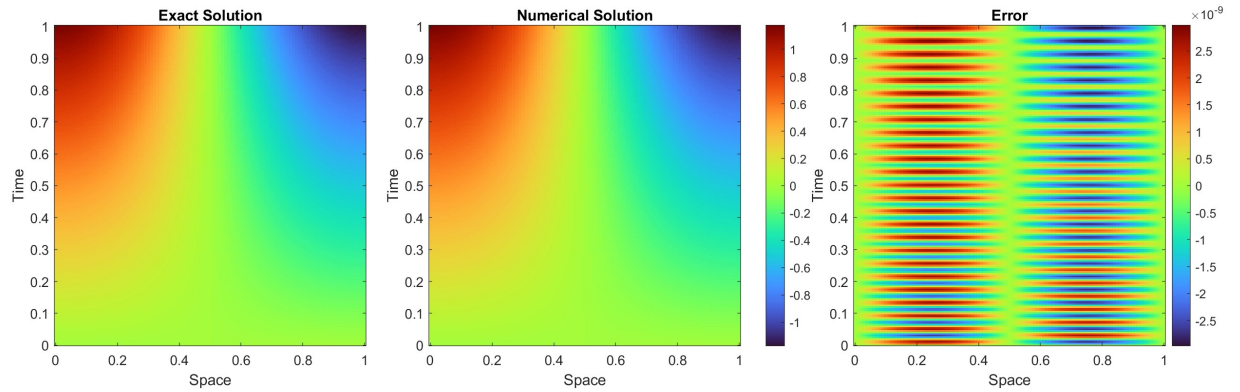
Table 2: Example 1: L^∞ errors for different values of h and $\Delta t = h^2$ at $t = 1$ Figure 2: Example 1: Error order with Δt of example 1Figure 3: Example 1: Error order with Δt of example 1

4.2 Example 2

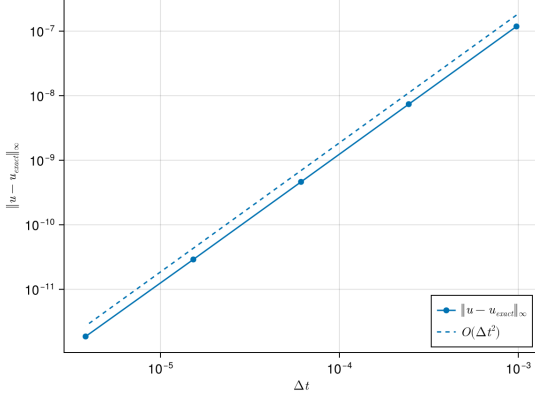
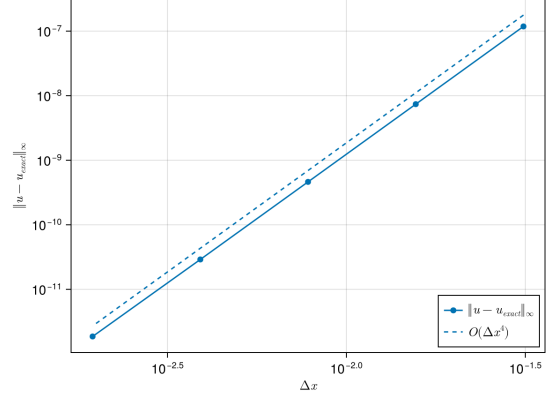
Example 2. Set $EI = 1, \rho = 1, c = 1$ in model (1) to (3) and the force term f is chosen such that exact solution is

$$u(x, t) = \sinh(t) \cos(\pi x). \quad (81)$$

The exact solution, numerical solution and error between exact and numerical solution, are plotted on 2D for $h = 0.01$ and $t = 0.005$ in fig 4. The maximum absolute errors in the solution variable u of example 2, are listed in Table 3 for different values of h at $t = 1$. Fig 4.2 and 4.2 show the convergence order of Example 2 in space and time, respectively.

Figure 4: Example 2: Exact solution (left), Numerical solution (middle) and Error (right) for $h = 0.01$ and $\Delta t = 0.005$

Mesh	N	h	e_h	C -order
$Mesh_1$	32	0.0312	1.182547729E-07	-
$Mesh_2$	64	0.0156	7.388819223E-09	4.000410771
$Mesh_3$	128	0.0078	4.620274163E-10	3.999293464
$Mesh_4$	256	0.0039	2.901023866E-11	3.993344393
$Mesh_5$	512	0.0020	1.859623566E-12	3.963479645
Average				3.989132068

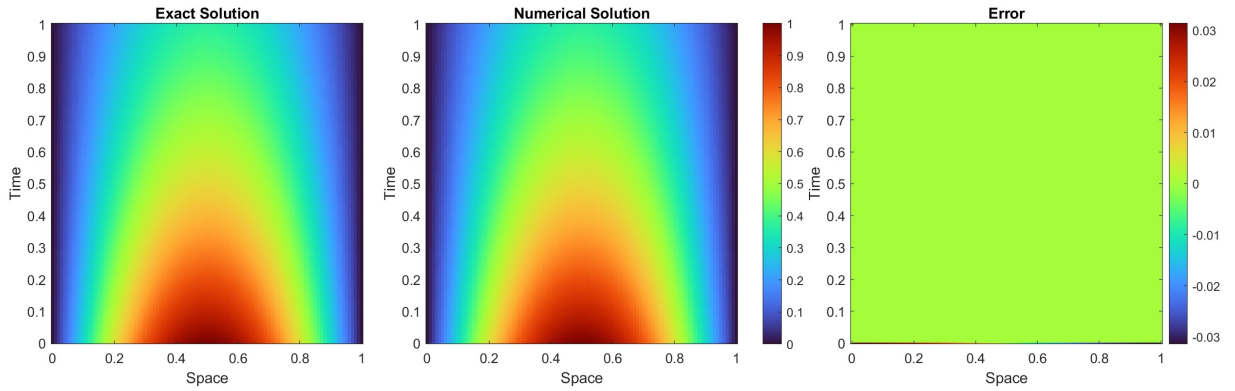
Table 3: Example 2: L^∞ errors for different values of h and $\Delta t = h^2$ at $t = 1$ Figure 5: Error order with Δt of example 2Figure 6: Error order with Δt of example 2

4.3 Example 3

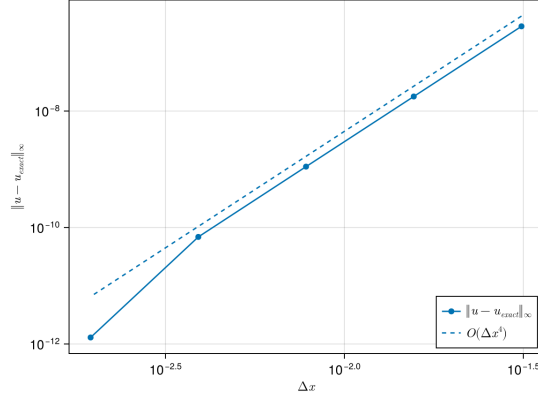
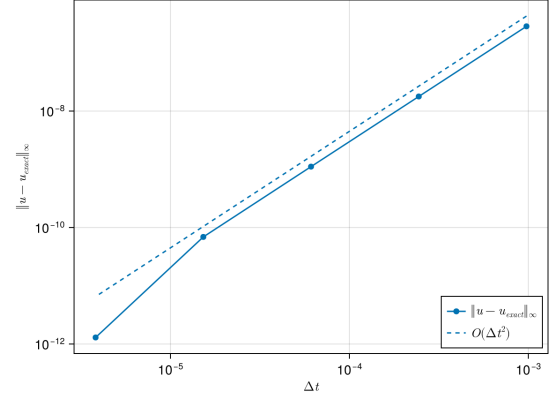
Example 3. Set $EI = 98$, $\rho = 0.68$, $c = 7.5$ in model (1) to (3) and the force term f is chosen such that exact solution is

$$u(x, t) = e^{-t} \sin(\pi x). \quad (82)$$

The exact solution, numerical solution and error between exact and numerical solution, are plotted on 2D for $h = 0.01$ and $t = 0.005$ in fig 7. The maximum absolute errors in the solution variable u of example 1, are listed in Table 4 for different values of h at $t = 1$. Fig 4.3 and 4.3 show the convergence order of Example 1 in space and time, respectively. In the error map, super-convergence occurs when either the time step or the spatial step is small enough, probably because the spatial and temporal steps satisfy a specific ratio making the error order higher.

Figure 7: Example 3: Exact solution (left), Numerical solution (middle) and Error (right) for $h = 0.01$ and $\Delta t = 0.005$

Mesh	N	h	e_h	C -order
$Mesh_1$	32	0.0312	2.849383778924519e-7	-
$Mesh_2$	64	0.0156	1.7771973226388127e-8	4.002974170882831
$Mesh_3$	128	0.0078	1.110404379556229e-9	4.000446804731633
$Mesh_4$	256	0.0039	6.894679271951532e-11	4.009457911233601
$Mesh_5$	512	0.0020	1.2934653348395386e-12	5.736170146624661
Average				4.437262258

Table 4: Example 3: L^∞ errors for different values of h and $\Delta t = h^2$ at $t = 1$ Figure 8: Error order with Δt of example 3Figure 9: Error order with Δt of example 3

5 Conclusion

In the numerical solution of the classic Euler-Bernoulli beam equation, this paper considers the case of constant coefficients after adding damping terms, and uses the fourth-order compact difference format and the Crank-Nicolson format finite difference method to solve it, solving the problem that damping terms are usually required in engineering. At the same time, this paper gives the consistency, stability and convergence proof of the compact finite difference method, and conducts a large number of numerical experiments to ensure the feasibility and universality of the method.

References

- [1] Clifford Ambrose Truesdell. *The rational mechanics of flexible or elastic bodies*. 1960.
- [2] Seon M Han, Haym Benaroya, and Timothy Wei. Dynamics of transversely vibrating beams using four engineering theories. *Journal of Sound and vibration*, 225(5):935–988, 1999.
- [3] Peng Li and Shiro Biwa. Flexural waves in a periodic non-uniform euler-bernoulli beam: analysis for arbitrary contour profiles and applications to wave control. *International Journal of Mechanical Sciences*, 188:105948, 2020.
- [4] Oliver A Bauchau and James I Craig. Euler-bernoulli beam theory. In *Structural analysis*, pages 173–221. Springer, 2009.
- [5] Jamil Abbas Haider, FD Zaman, Showkat Ahmad Lone, Sadia Anwar, Salmeh A Almutlak, and Ibrahim E Elseesy. Exact solutions of euler-bernoulli beams. *Modern Physics Letters B*, 37(33):2350161, 2023.
- [6] Abdarrhim M Ahmed and Abdussalam M Rifai. Euler-bernoulli and timoshenko beam theories analytical and numerical comprehensive revision. *European Journal of Engineering and Technology Research*, 6(7):20–32, 2021.
- [7] Valentin Fogang. Euler-bernoulli beam theory: First-order analysis, second-order analysis, stability, and vibration analysis using the finite difference method, 2021.
- [8] EH Twizell and AQM Khaliq. A difference scheme with high accuracy in time for fourth-order parabolic equations. *Computer methods in applied mechanics and engineering*, 41(1):91–104, 1983.

- [9] Atilla Özütok and Arife Akin. The solution of euler-bernoulli beams using variational derivative method. *Scientific Research and Essays*, 5(9):1019–1024, 2010.
- [10] J Awrejcewicz, AV Krysko, J Mrozowski, OA Saltykova, and MV Zhigalov. Analysis of regular and chaotic dynamics of the euler-bernoulli beams using finite difference and finite element methods. *Acta Mechanica Sinica*, 27:36–43, 2011.
- [11] Ranjan Kumar Mohanty and Deepti Kaur. High accuracy compact operator methods for two-dimensional fourth order nonlinear parabolic partial differential equations. *Computational Methods in Applied Mathematics*, 17(4):617–641, 2017.
- [12] Jarkko Niiranen, Viacheslav Balobanov, Josef Kiendl, and SB3894509 Hosseini. Variational formulations, model comparisons and numerical methods for euler-bernoulli micro-and nano-beam models. *Mathematics and Mechanics of Solids*, 24(1):312–335, 2019.
- [13] Maheshwar Pathak and Pratibha Joshi. High-order compact finite difference scheme for euler-bernoulli beam equation. In *Harmony Search and Nature Inspired Optimization Algorithms: Theory and Applications, ICHSA 2018*, pages 357–370. Springer, 2019.
- [14] My Driss Aouragh, Yassin Khali, Samir Khallouq, and M’hamed Segauoi. Compact finite difference scheme for euler-bernoulli beam equation with a simply supported boundary conditions. *International Journal of Applied and Computational Mathematics*, 10(1):17, 2024.
- [15] NS Bardell. An engineering application of the hp version of the finite element method to the static analysis of a euler-bernoulli beam. *Computers & structures*, 59(2):195–211, 1996.
- [16] Dongming Wei and Yu Liu. Analytic and finite element solutions of the power-law euler-bernoulli beams. *Finite Elements in Analysis and Design*, 52:31–40, 2012.
- [17] MA Eltaher, Amal E Alshorbagy, and FF3020612 Mahmoud. Vibration analysis of euler-bernoulli nanobeams by using finite element method. *Applied Mathematical Modelling*, 37(7):4787–4797, 2013.
- [18] Ngoc-Tuan Nguyen, Nam-Il Kim, and Jaehong Lee. Mixed finite element analysis of nonlocal euler-bernoulli nanobeams. *Finite Elements in Analysis and Design*, 106:65–72, 2015.
- [19] HY Shang, RD Machado, and JE Abdalla Filho. Dynamic analysis of euler-bernoulli beam problems using the generalized finite element method. *Computers & Structures*, 173:109–122, 2016.
- [20] Mohammad Zakeri, Reza Attarnejad, and Amir Mohsen Ershadbakhsh. Analysis of euler-bernoulli nanobeams: A mechanical-based solution. *Journal of Computational Applied Mechanics*, 47(2):159–180, 2016.
- [21] Min Lin, Tao Lin, and Huili Zhang. Error analysis of an immersed finite element method for euler-bernoulli beam interface problems. *International Journal of Numerical Analysis & Modeling*, 14(6), 2017.
- [22] Yongliang Wang, Yang Ju, Zhuo Zhuang, and Chenfeng Li. Adaptive finite element analysis for damage detection of non-uniform euler-bernoulli beams with multiple cracks based on natural frequencies. *Engineering Computations*, 35(3):1203–1229, 2018.
- [23] APGOH ABRO, JM Gossrin Bomisso, A KIDJÉGBO TOURÉ, and Adama Coulibaly. A numerical method by finite element method (fem) of an euler-bernoulli beam to variable coefficients. *Adv. Math. Sci. J*, 9:8485–8510, 2020.
- [24] Guilin Sun and Christopher W Trueman. Efficient implementations of the crank-nicolson scheme for the finite-difference time-domain method. *IEEE transactions on microwave theory and techniques*, 54(5):2275–2284, 2006.
- [25] Eric W Weisstein. Gershgorin circle theorem. <https://mathworld.wolfram.com/>, 2003.
- [26] Peter D Lax and Robert D Richtmyer. Survey of the stability of linear finite difference equations. In *Selected Papers Volume I*, pages 125–151. Springer, 2005.